e-Navi

Available online at http://www.e-navigation.kr/
e-Navigation Journal

Original article

SOC Modelling and Simulation of Lithium-Sulfur Battery Equivalent Circuit

Zhengrui Zhang[a], Mingyu Wang[a*], Qianyong Zhang[a,b], Zhe Gao[a]

[a*] International Maritime Academy, Hainan Tropical Ocean University, Sanya, China, 15591465471@163.com

[b] Maritime College, Shandong Jiaotong University, Weihai, Shandong, China, 2009zqy@163.com

Abstract

Electric-propulsion systems for ships, also known as electric propulsion devices, represent the current direction of development for maritime power. Issues concerning the environment and fuel economy have compelled the maritime transport sector to seek solutions that reduce emissions and improve fuel efficiency. In this process, power electronics technology plays a significant role in the propulsion systems of ships. Selecting an efficient battery system is of great importance for enhancing the cruising range of yachts and minimizing environmental impact. The battery model is crucial for revealing the working principles of batteries, and it is extremely critical for the application and development of battery technology. The Battery Management System (BMS) serves a crucial regulatory function, optimizing both the safety and performance of battery cells. Central to its operation is the precise estimation of the battery's State of Charge (SOC), a process dependent on an exacting battery model. This system not only enhances longevity and reliability but also ensures that energy storage solutions meet high standards of efficacy. This study focused on testing the impedance characteristics of lithium-sulfur batteries (LSB) at various SOC points and establishing first- and second-order RC equivalent circuit models. The model parameters were identified through experimental data. Subsequently, a simulation platform was constructed using MATLAB/Simulink to simulate the behavior of LSB under a constant current discharge condition. The simulation results showed that the second-order RC model had significantly lower errors than the first-order model, demonstrating higher accuracy. These achievements can provide technical support for the research of energy storage systems in the green aviation and maritime industries.

Keywords: Ship Electric Propulsion System, SOC,Impedance Characteristics, Equivalent Circuit Model, Simulation

https://doi.org/10.52820/j.enavi.2024.22.034

1. Introduction

Main text With economic development, leisure yachts aimed at the general public have begun to attract attention, gradually becoming the new driving force for the development of the yacht market[1]. Currently, China's yacht industry is in a stage of rapid growth, showing a remarkable momentum. This industry has not only driven the prosperity of the yacht manufacturing industry but also given birth to the rise of many related industries[2].With the rapid growth of the yacht industry, it will continue to make a positive contribution to the development of the national economy and the diversification of consumer demand in the future. Battery technology plays a critical role in the modern yacht manufacturing industry as it directly influences the endurance performance of yachts and their environmental impact. With the advancement of eco-friendly energy technology, many yachts have turned to the use of clean energy. These energy systems not only provide clean power, ensuring the reliability and safety of navigation, but also protect the marine environment. LSB technology, known for its excellent energy density, utilizes the widely available and low-cost sulfur resources on Earth. This type of battery is considered to be a promising green energy storage technology due to its environmental compatibility and high energy storage efficiency, which can improve the efficiency of clean energy use and reduce greenhouse gas emissions. Therefore, choosing an efficient battery system is of great significance for increasing the sailing distance of the yacht and reducing environmental impact [3].The battery model is the link to understanding the working mechanism of batteries, capturing the characteristics of rechargeable batteries through a dynamic parameterization process, which is of great significance in promoting the application and progress of battery technology.

BMS can optimize battery performance by accurately monitoring the battery status, ensuring its safety, and extending its working life as much as possible. As the intelligent supervisory center for the battery, the BMS monitors and maintains the state of each battery cell within the battery pack, ensuring they work safely and efficiently. The main responsibility of the BMS is to prevent overcharging or over-discharging of the battery, which can maintain battery health, and ensure efficiency and stability during the charging and discharging process. The basic functions of the BMS include executing state monitoring, safety monitoring, performance testing, and data information management, among which, accurately estimating the battery's SOC is its core responsibility. To achieve this goal, the BMS must perform precise SOC estimation based on a highly accurate battery model. Electrochemical models, due to the involvement of numerous differential equations, result in a large number of unknown parameters that need to be identified, making them unsuitable for real-time online BMS applications[4]. For LSB, data-driven models also face the challenge of improving accuracy when dealing with their complex operating conditions[5].LSB trigger a series of complex electrochemical reactions during charging and discharging, which are closely related to the battery's internal resistance and directly connected to the battery's SOC. Therefore, by analyzing the interrelationship between the battery's internal impedance characteristics and its state, the SOC of LSB can be effectively estimated. Equivalent circuit models provide an intuitive representation of the internal dynamic chemical behavior by simulating the physical phenomena in the electrochemical process. These models successfully integrate electrochemical theory with circuit analysis, endowing the model parameters with practical application value. For LSB, by correlating their internal impedance characteristics with the battery state, the state of the battery can be effectively estimated. This method has been widely used in the state assessment and impedance characteristic analysis of lithium-ion batteries, and the impedance spectrum obtained from electrochemical tests can be accurately fitted using equivalent circuit models. Different circuit structures reflect the diverse physical processes in electrochemical reactions, further confirming the importance of combining electrochemistry with circuitry in constructing equivalent circuit models with practical significance.

Extensive research efforts are currently devoted to exploring the interconnection between electrical resistance, charge exchange resistance, diffusional impedance, and diverse elements including the battery's SOC, its State of Health (SOH), ambient temperature, and the dynamics of charging and discharging rates. These studies aim to provide comprehensive explanations based on electrochemical principles. Research has found that the organic integration of

electrochemical theory with circuit science endows the parameters of the constructed equivalent circuit models with practical application value. For the complex operating conditions of LSB, it is challenging for data-driven models to improve the accuracy of the models. Susana Chauque and colleagues' research (2024) has revealed the positive impact of the interaction between polysulfides and PPY on enhancing the performance of LSB[6]. In their extensive research published in 2023, Érick A. Santos and his team delved into the electrochemical attributes of LSB [7]. Utilizing an array of methodologies such as scanning electron microscopy, cyclic voltammetry, alternating current impedance, and charge-discharge cycling, they meticulously examined and interpreted the operational dynamics of these batteries. In 2024, Seyed-Morteza Hoseyni and colleagues proposed a novel approach for system identification using admittance, which ensures the precise and stable estimation of equivalent circuit parameters in the modeling process of piezoelectric energy harvesters integrated with plate structures [8]. This method allows for the intuitive visualization of the dynamics of electrochemical reaction processes. Alan G. Li (2023) proposed a new method for degradation diagnosis in battery management systems by utilizing pulse response to reflect the internal dynamics parameters and electrode phase changes of the battery [9]. Haichi Huang (2024) proposed a SOC-SOH estimation framework that can accurately estimate the health status and charge status of lithium-ion batteries throughout their entire lifecycle [10].Dini P (2024) conducted an in-depth analysis of current battery SOC estimation methods and algorithms, emphasizing their key role in the power electronics of vehicles and mechatronics systems[11]. Çarkıt T et al. (2024) utilized optimization algorithms to the Thevenin equivalent circuit model of batteries to achieve highly accurate estimation of the open-circuit voltage and battery health status [12]. Watanabe H et al. (2024) conducted an analysis of LSB through in-situ electrochemical impedance spectroscopy testing, which not only allowed for an in-depth exploration of their reaction kinetics mechanism but also effectively optimized the performance of the batteries [13]. Zabara M A et al. (2024) utilized temperature-dependent electrochemical impedance spectroscopy (EIS) technology to deeply analyze the charge transfer dynamics of lithium batteries[14]. By adjusting key parameters during the EIS testing process, they were able to associate the observed charge transfer resistance with specific electrochemical processes, thereby accurately obtaining the kinetic parameters of these processes. This study highlights the unique advantages of EIS technology in analyzing the complex charge transfer phenomena within lithium batteries. Babaeiyazdi I et al. (2021) employed EIS data, combined with machine learning models, to accurately predict the SOC of lithium-ion batteries [15]. Through model training, they achieved a result where the model's prediction error was below 3.8%. Li C et al. (2024) proposed an equivalent circuit model and a data-driven method based on electrochemical impedance spectroscopy (EIS) for estimating the SOH of lithium-ion batteries (LIBs), achieving an average estimation error as low as 1.77% [16]. Li F (2024) proposed a circuit model for batteries and used an algorithm to accurately identify the parameters of the circuit model [17]. The root mean square error and maximum error of this method were both less than 1.8% and 7.65%, respectively. Zhao J et al. (2024) proposed a parameterized mathematical model to achieve more accurate predictions and state tracking for battery performance [18]. Tolouei N E et al. (2020) utilized EIS technology to construct a circuit model for biosensors, and conducted a detailed analysis of circuits of varying complexity and equivalent circuits across a range of frequencies [19]. Lipu M S H et al. (2022) provided a comprehensive review based on deep learning for the precise estimation of key parameters in electric vehicles (EVs), and put forward prospects to promote the development of intelligent BMS[20].

This article uses a LSB manufactured in the laboratory as the research object, applies the theoretical methods of electrochemical performance analysis, and conducts an in-depth analysis of its impedance characteristics at different SOC points. Based on this, first and second-order RC equivalent circuit models were constructed. By applying experimental data to the model, parameter identification was successfully carried out, thereby completing the model construction. Furthermore, a simulation environment was built using MATLAB/Simulink software to simulate and verify the behavior of the LSB under constant current discharge conditions.

2. EIS and Basic Theory of Equivalent Elements

2.1 Basic Theory of EIS

EIS is an advanced analytical technique used to investigate the internal dynamics of electrochemical systems. By analysing the impedance variation with frequency under an alternating current (AC) electric field, it reveals important characteristics such as electro kinetics, electrode interface structure, and mass transfer. The advantage of EIS lies in its use of a small amplitude AC signal to avoid disturbing the system's equilibrium state.

The essence of EIS lies in measuring the ratio between the perturbation signal and the response signal Y at different frequencies o(f). These data, when expressed graphically, help to gain an in-depth understanding of the electrode processes, double-layer characteristics, and diffusion mechanisms of the battery system.

To accurately assess the frequency response of an electrochemical system, EIS must meet three basic conditions: the system's causality, linearity, and stability during the measurement process. Causality refers to the system's output response being caused by the input signal, meaning the system's response cannot occur without the corresponding input, nor can it appear before the input signal. Linearity indicates that the input and output signals in the electrochemical system should exhibit linearly changing characteristics Consequently, it suggests that upon encountering a minor AC signal disturbance, the system's reaction ought to maintain linearity, meaning the output signal's magnitude is directly comparable to the input signal's intensity.Stability indicates that during the EIS testing process, the parameters within the electrochemical system under study should not change over time, including the system being in a steady state rather than a transient one, and that system parameters do not vary with the passage of time.

2.2 Basic Theory of Equivalent Elements

Equivalent circuits are composed of basic circuit elements, connected in series or in parallel. The selection of an equivalent circuit is based on its impedance characteristics matching those of the target battery, enabling it to simulate the electrochemical properties of the battery. Such a circuit can serve as a simulation model for the battery, assisting in an in-depth analysis of the battery's electrochemical reactions. Each component in the equivalent circuit, known as an equivalent element, corresponds to a specific electrochemical action and physical state within the battery. Common equivalent elements include the equivalent resistor R, equivalent capacitor C, equivalent inductor L, and constant phase element Q, among others.

3. Establishing Equivalent Circuit Models for LSB

3.1 EIS Experiment

The battery's State of Charge (SOC) represents the residual capacity left, commonly quantified by the electrical energy either used up or released through charging or discharging processes.

$$SOC = 1 - \frac{Q}{C_Q} \tag{1.1}$$

Within the equation, Q denotes the instantaneous electricity consumption of the battery, while C_Q stands for the current actual capacity of the battery. SOC (State of Charge) reflects the battery's charging status, with a range valued between 0 and 1, often expressed as a percentage. A SOC of 0 implies that the battery has been entirely depleted, whereas a SOC of 1 suggests a complete charge.

Currently, there are several methods available for estimating SOC in batteries. The Ah-integration method relies on the integration of the battery's charging and discharging current over time. This method is universally applicable to all types of batteries and is not limited to specific battery types. The OCV method depends on the stable voltage value measured after the battery has been fully at rest, and the SOC value is estimated by fitting with a preset voltage-SOC curve. The constant current discharge test method determines the remaining battery capacity by multiplying the discharge current with time at a constant current until a specific condition is reached. This method is suitable for all types of batteries. In this article, the discharge experiment method is used as a means of SOC estimation.

EIS data is the key foundation for constructing equivalent circuit models, which need to be obtained

through a specific testing process. The following are the steps for EIS testing of the battery to establish a model:

(1) Select a battery and let it rest for 24 hours to ensure it reaches a stable state. Under the specified test conditions, perform charge and discharge cycles at a current density of 0.1C until the battery reaches a stable capacity C_Q, which will serve as the reference capacity for the battery.

(2) Continue to charge the battery at a current density of 0.1C to a voltage level of 2.8V, then let the battery rest again for 1 hour to ensure the consistency of the battery state.

(3) After the battery has rested, perform EIS testing to obtain the impedance spectrum data of the battery in its current state.

(4) Discharge the battery at a current density of 0.1C, reducing the SOC by 10% each time, and then let the battery rest for another 1 hour to obtain the battery's impedance characteristics at different SOC states.

(5) Repeat the EIS testing at each point where the SOC is reduced by 10%, collecting the battery impedance data at different states, which will be used for subsequent equivalent circuit model establishment and parameter fitting.

Repeat steps (4) and (5) for each SOC measurement point until EIS testing is completed for all points. The EIS impedance spectrum diagrams of all SOC states obtained from the test are shown in the following Figure 1. When the SOC changes, the high-frequency segment of EIS does not change much, indicating that the ohmic resistance R_0 does not show significant changes. The arc at the medium frequency stage increases as the SOC decreases, indicating that the charge transfer impedance increases as the SOC decreases.

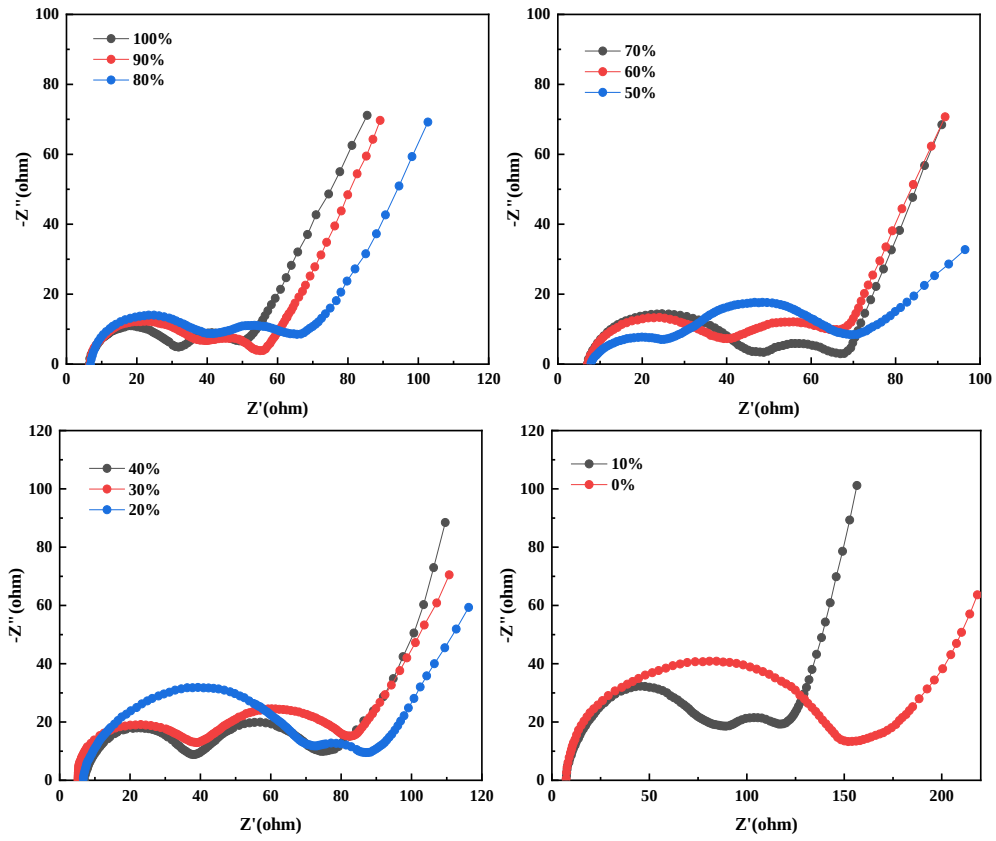

Figure 1 Impedance Spectrum Diagram of LSB at Various SOC Points

3.2 Establishing an Equivalent Circuit Model

An equivalent circuit model is employed, integrating circuit components alongside EIS data to decipher the battery's internal electrochemical mechanisms and charge exchange characteristics. At high frequencies, the circuit mimics the anode material's activation process through the parallel combination of R_{sf} resistance and C_{sf} capacitance,

forming the arc segment. Moving to the medium-frequency range, the arc is symbolized by R_{ct} resistance and C_{ct} capacitance in parallel, reflecting the cathode's activation dynamics. In the low-frequency domain, the straight line with a 1-unit slope is simulated by a CPE, while the Warburg impedance, Z_w, captures the mass transport phenomena within the battery. These electrochemical processes find expression in the various elements of the EIS equivalent circuit diagram. As shown in Figure 2, the ohmic resistance, R_0 , intersects the real axis at the highest frequency point manifesting as a solitary point on the real axis, independent of frequency variations.

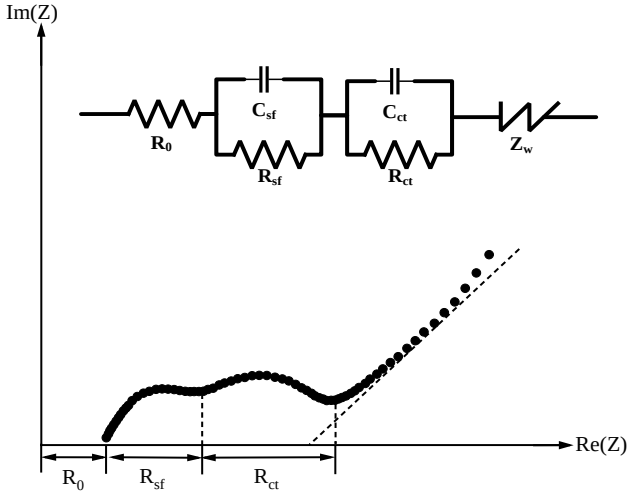

Figure 2 Electrochemical impedance spectroscopy plot and its corresponding equivalent circuit

Each frequency band's impedance profile can be depicted through an equivalent circuit representation. At the higher frequency end, the point where it intersects with the real axis denotes the battery's constant ohmic resistance, denoted as R_0. This resistance value stays unaffected by the frequency variations. The impedance formulation for R_0 is :

$$Z_R(\omega) = R_0 \tag{1.2}$$

In the formula: ω represents the frequency of the alternating current signal.

According to Equation (1.3), the parallel combination of equivalent resistance and equivalent capacitance can be represented through an altered impedance formulation as:

$$Z_{RC}(\omega) = \frac{R}{1+(\omega RC)^2} - j\frac{\omega R^2 C}{1+(\omega RC)^2} = \frac{R}{1+\omega^2\tau^2} - j\frac{\omega\tau R}{1+\omega^2\tau^2} \tag{1.3}$$

Within the equation, the time constant τ signifies the pace of the reaction mechanism. Thus, the anode activation kinetics impedance Z_{sf} can be articulated as:

$$Z_{sf}(\omega) = \frac{R_{sf}}{1+\omega^2\tau_{sf}^2} - j\frac{\omega\tau_{sf}R_{sf}}{1+\omega^2\tau_{sf}^2} \tag{1.4}$$

The cathode activation dynamics impedance Z_{ct} is:

$$Z_{ct}(\omega) = \frac{R_{ct}}{1+\omega^2\tau_{ct}^2} - j\frac{\omega\tau_{ct}R_{ct}}{1+\omega^2\tau_{ct}^2} \tag{1.5}$$

The Warburg resistance impedance Z_w is:

$$Z_w(\omega) = \frac{\sigma}{\sqrt{\omega}}(1-j) = \sigma\omega^{-\frac{1}{2}} - j\sigma\omega^{-\frac{1}{2}} \tag{1.6}$$

In the formula, σ represents the lithium ion conductivity in LSB.

Upon streamlining the battery model, the insignificant effect of the Warburg impedance at low frequencies on the overall modeling precision is taken into account, leading to its exclusion in this analysis. As depicted in Figure 3, the adopted simplified model is a second-order RC equivalent circuit. This circuit effectively omits the Warburg impedance yet maintains an accurate depiction of the battery's dynamic behavior.

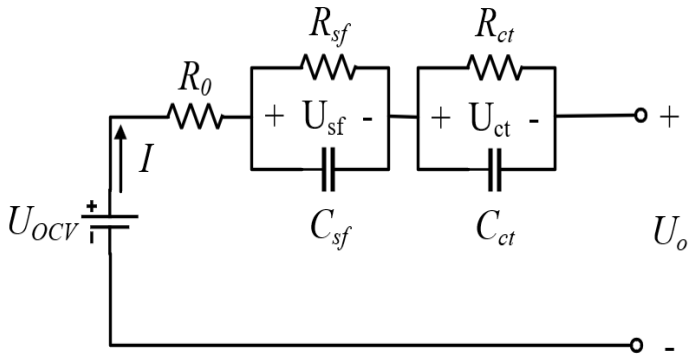

Figure 3 Second-order RC equivalent circuit model

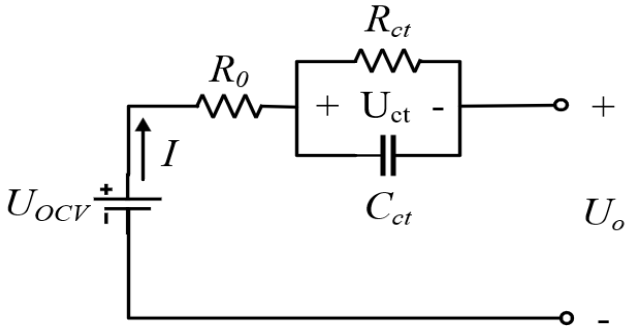

Figure 4 First-order RC equivalent circuit model

By considering the capacitor voltages U_{sf} and U_{ct} as state variables, the derivation of the time-domain second-order RC equivalent circuit's ordinary differential equation unfolds as follows:

$$\begin{cases} U_o = U_{ocv} - U_{sf} - U_{ct} - IR_0 \\ \dot{U}_{ct} = \dfrac{I}{C_{ct}} - \dfrac{U_{ct}}{R_{ct}C_{ct}} \\ \dot{U}_{sf} = \dfrac{I}{C_{sf}} - \dfrac{U_{sf}}{R_{sf}C_{sf}} \end{cases} \tag{1.7}$$

By virtue of a redesigned separator that mitigates polysulfide intrusion onto the anode, the complexity of the second-order RC equivalent circuit model can be diminished by excluding the anode activation behavior represented by the C_{sf} and C_{sf} parallel components. For purposes of comparison, a first-order RC equivalent circuit is also established, as illustrated in Figure 4, to model the LSB. Though simplifying the internal architecture of the first-order model enhances ease of use and computational efficiency, it potentially compromises precision. Herein, two distinct RC equivalent circuit models are chosen for LSB representation. A subsequent analysis and comparison of their fitting outcomes will be conducted to identify the optimal circuit model for accurately capturing the battery's behavior.

Regarding the capacitor voltage, U_{ct}, as the state variable, we can formulate the time-domain ordinary differential equation governing the first-order RC circuit as follows:

$$\begin{cases} U_o = U_{ocv} - U_{ct} - IR_0 \\ \dot{U}_{ct} = \dfrac{I}{C_{ct}} - \dfrac{U_{ct}}{R_{ct}C_{ct}} \end{cases} \tag{1.8}$$

4. Parameter Identification for LSB Model

4.1 Open-Circuit Voltage Parameter Identification

Given that the cell potential connected to SOC isn't directly measurable, the open-circuit voltage, denoted as U_{ocv}, is typically employed as an indirect indicator.It is generally believed that when the battery is disconnected from the load and allowed to rest for a sufficient period, the stable voltage at the battery terminals is U_{ocv}. The relationship between a battery's internal SOC parameter and its external voltage output is crucially depicted in the U_{ocv}-SOC curve, which also enables forecasting the open-circuit voltage at a given SOC level. To discern the distinctive traits of this curve for LSB, one follows these testing procedures:

(1) Allow the selected battery to rest for 24 hours, then perform charge and discharge cycles at a current density of 0.1C under specified test conditions until 10 cycles are completed. The battery capacity recorded at this time is defined as C_Q.

(2) Continue to charge the battery at a current density of 0.1C to a voltage level of 2.8 V, then rest for another hour to ensure the stability of the battery's internal state.

(3) During the discharge process at a current density of 0.1C, we halted the discharge whenever the SOC decreased by 10% and recorded the corresponding battery voltage at that point.

Repeat step 3 until voltage data at all SOC measurement points are obtained. The purpose of resting for one hour is to allow the internal state of the battery to stabilize and ensure the accuracy of the voltage reading. As shown in Figure 5, the U_{ocv}-SOC curve of LSB under a charge and discharge rate of 0.1C typically shows that the voltage platform is relatively flat when the SOC is between 20% and 60%, while the voltage drops more rapidly in other SOC ranges. Guaranteeing the robustness of battery performance necessitates operating it within an SOC (State of Charge) window spanning from 20% to 60%.

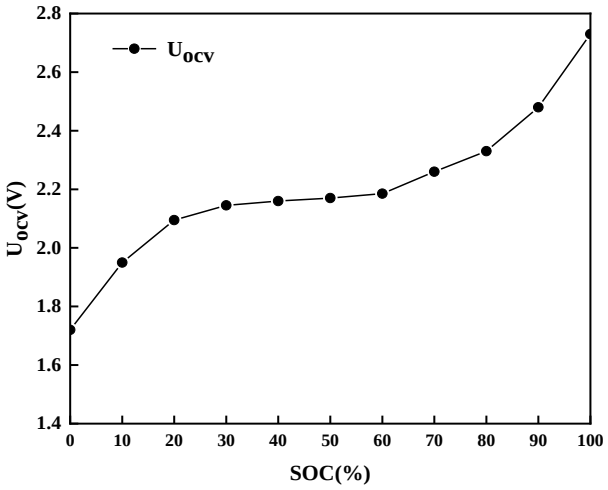

Figure 5 U_{ocv}-SOC Characteristic Curve

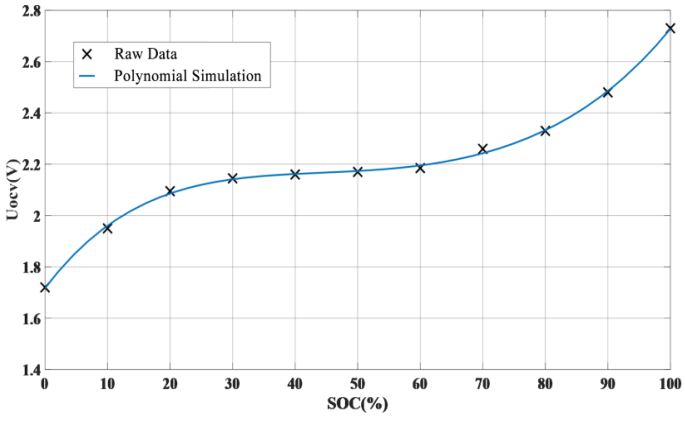

Figure 6 U_{ocv}-SOC Fitting Curve

For enhancing precision and streamlining the representation, we employed MATLAB's cftool for curve-fitting to establish the functional correlation between U_{ocv} and SOC as outlined in Equation (1.9).

$$U_{ocv} = a_0 + a_1 SOC + a_2 SOC^2 + a_3 SOC^3 + \cdots + a_n SOC^n \quad (1.9)$$

A fifth-degree polynomial function is selected for

fitting, and the fitting result is shown in Figure 6. The expression of the fitting curve is as follows, with an R-square value of 0.99803.

$$U_{ocv} = 1.717 + 0.03231 \times SOC - 0.0009086 \times SOC^2 + (1234e-05) \times SOC^3 - (8.279e-08) \times SOC^4 + (2.804e-10) \times SOC^5 \quad (1.10)$$

4.2 Parameter Identification for First-Order RC Model

Using the impedance expressions of equivalent elements to calculate the equivalent circuit element parameter values at each SOC point (as shown in Table 1). Figure 7 illustrates the impedance spectrum associated with the first-order RC equivalent circuit.

By utilizing the RC impedance expression, we can derive the magnitude expression for the first-order RC impedance as follows:

$$Z = R_0 + \frac{1}{j\omega C_{ct} + R_{ct}^{-1}} = R_0 + \frac{R_{ct}}{1+\omega^2 R_{ct}^2 C_{ct}^2} - j\frac{\omega R_{ct}^{\ 2} C_{ct}}{1+\omega^2 R_{ct}^2 C_{ct}^2} \quad (1.11)$$

In the realm of complex frequencies, the modulus of the impedance takes on the form of a semi-circle with a span equal to R_{ct}, which is mathematically expressed as:

$$\left(Z' - R_0 - \frac{R_{ct}}{2}\right)^2 + Z''^2 = \left(\frac{R_{ct}}{2}\right)^2 \quad (1.12)$$

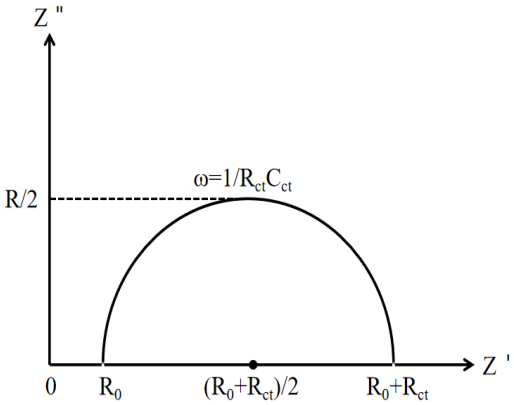

Figure 7 Impedance spectrum diagram of the first-order RC circuit

The parameters of the initial-order RC equivalent circuit can be inferred from the EIS experimental data previously analyzed. The parameter R_0 is equivalent to the magnitude on the real axis where the initial semi-circle's starting point intersects. To determine R_{ct}, subtract R_0 from the magnitude where the semi-circle's ending point meets the real axis. Furthermore, by identifying the angular frequency ω'' that corresponds to the apex of the semi-circle's center, and utilizing the derived R_{ct} and ω'', the capacitance C_{ct} can be computed using a specific equation.

$$C_{ct} = \frac{1}{\omega * R_{ct}} \quad (1.13)$$

Table 1: First-Order RC Model Parameter Identification Results

SOC	0	10%	20%	30%	40%	50%	60%	70%	80%	90%	100%
R_0(Ω)	7.34	7.31	6.72	5.21	7.13	7.84	7.03	6.97	6.85	6.65	6.48
R_{ct}(Ω)	143.15	29.51	17.26	45.33	38.42	44.88	27.86	20.95	25.87	17.85	18.14
C_{ct}(mF)	0.002	0.854	0.184	0.176	0.165	0.178	0.286	0.190	0.154	0.224	0.220

4.3 Parameter Identification of the Second-Order RC Model

Based on the impedance expression of the first-order RC equivalent circuit, the impedance magnitude of the second-order RC equivalent circuit is derived, expressed as:

$$Z = R_0 + \frac{1}{j\omega C_{ct} + R_{ct}^{-1}} + \frac{1}{j\omega C_{sf} + R_{sf}^{-1}}$$
$$= R_0 + \frac{R_{ct}}{1+\omega^2 R_{ct}^2 C_{ct}^2} + \frac{R_{sf}}{1+\omega^2 R_{sf}^2 C_{sf}^2} - j\left(\frac{\omega R_{ct}{}^2 C_{ct}}{1+\omega^2 R_{ct}^2 C_{ct}^2} + \frac{\omega R_{sf}{}^2 C_{sf}}{1+\omega^2 R_{sf}^2 C_{sf}^2}\right) \quad (1.14)$$

In the realm of complex frequencies, the impedance expression for the initial semi-circle of the second-order RC circuit's impedance spectrum can be depicted as a circular arc with a radius equivalent to R_{sf} divided by 2, formulated as follows:

$$\left(Z' - R_0 - \frac{R_{sf}}{2}\right)^2 + Z''^2 = \left(\frac{R_{sf}}{2}\right)^2 \quad (1.15)$$

Identify the angular frequency that corresponds to the peak located at the midpoint of the semicircle as ω'. Upon extracting R_{sf} and ω' from the spectral diagram, utilize the subsequent equation to calculate C_{sf}:

$$C_{sf} = \frac{1}{\omega' R_{sf}} \quad (1.16)$$

The second semicircular impedance can be depicted as a circle divided in half, having a radius equal to R_{ct} divided by two. Its mathematical representation is as stated below:

$$\left(Z' - R_0 - R_{sf} - \frac{R_{ct}}{2}\right)^2 + Z''^2 = \left(\frac{R_{ct}}{2}\right)^2 \quad (1.17)$$

Set the angular frequency corresponding to the highest point at the center of the semicircle as ω''. After obtaining R_{sf}, R_{ct}, and ω'' from the spectrum graph, C_{ct} can be derived using the following formula:

$$C_{ct} = \frac{1}{\omega'' R_{ct}} \quad (1.18)$$

Employing experimental data and the impedance spectra representations of equivalent components, we undertook model parameter determination for a second-order RC equivalent circuit at various SOC phases. Upon contrasting the parameter identification outcomes of the first-order RC model with those of the second-order RC model, it becomes clear that the parameters of each constituent element exhibit variations across distinct SOC stages, thereby revealing an inconsistency pattern.

To enhance the accuracy of the equivalent circuit model and simplify the algorithm, it is important to establish functional relationships between the parameters of each element and SOC. By simplifying the R_{sf} and C_{sf} of the second-order RC equivalent model, we obtain the first-order RC equivalent model, ensuring consistency in relevant values and functional relationships.

Employing MATLAB's cftool for curve fitting, the coefficients for various functional relationships are established. Upon insertion of these coefficients into the respective relational formulas, the equations connecting the component parameters with SOC are derived, as expressed from (1.19) through (1.23).

$$R_0(SOC) = 7.472 - 2.041\times SOC - 45.92\times SOC^2 + 209.8\times SOC^3 - 289.2\times SOC^4 + 126.4\times SOC^5 \quad (1.19)$$

$$R_{sf}(SOC) = 141 - 622.9\times SOC + 1059\times SOC^2 - 480.8\times SOC^3 + 175.9\times SOC^4 + 103\times SOC^5 \quad (1.20)$$

$$C_{sf}(SOC) = 1.862 + 3.232\times SOC + 61.13\times SOC^2 - 223.9\times SOC^3 + 245\times SOC^4 - 86.06\times SOC^5 \quad (1.21)$$

$$R_{ct}(SOC) = 141.9 - 1891\times SOC + 9947\times SOC^2 - (2.17e+04)\times SOC^3 + (2.08e+04)\times SOC^4 - (7.27e+03)\times SOC^5 \quad (1.22)$$

$$C_{ct}(SOC) = 0.06996 + 11.64\times SOC - 81.56\times SOC^2 + 204\times SOC^3 - 214.1\times SOC^4 + 80.19\times SOC^5 \quad (1.23)$$

In addition, the root mean square error (RMSE) and the coefficient of determination (R-square) are important indicators for judging the goodness of curve fitting. The smaller the RMSE and the closer R-square is to 1, the better the curve fitting effect.

From the two evaluation indicators in Table 2, it can be seen that the fitting results of each functional relationship formula are very excellent.

Table 2 Various Evaluation Indicators of the Fitted Model Parameters

Evaluation Indicators	R_0	R_{sf}	C_{sf}	R_{ct}	C_{ct}
R-square	0.3915	0.9546	0.7026	0.9528	0.593
RMSE	0.7349	7.737	0.6835	7.829	0.4341

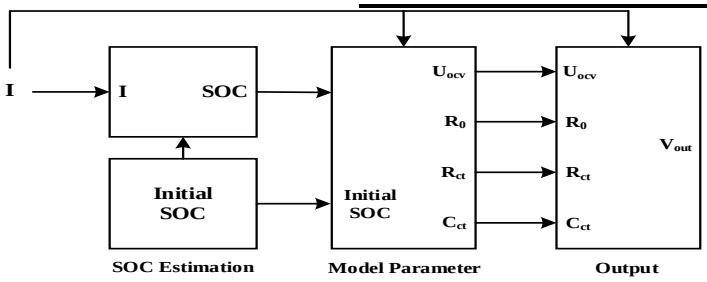

Figure 8 Schematic diagram of the first-order RC equivalent circuit model simulation platform

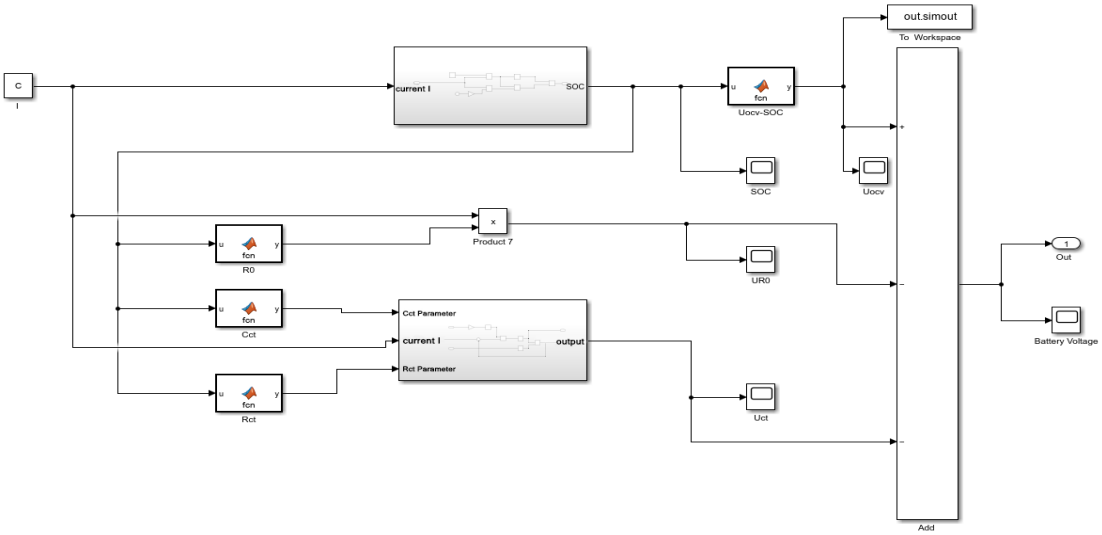

Figure 9 Schematic diagram of the first-order RC equivalent circuit model simulation platform

5. Model Simulation Platform Construction

5.1 Construction of the First-Order RC Model Simulation Platform

The structural diagram of the first-order RC equivalent circuit model simulation platform is shown in Figure 8, where each module corresponds to different functions, and the main modules include the SOC estimation module, model parameter module, and output verification module.

Before constructing the simulation platform of the first-order RC equivalent circuit model in MATLAB/Simulink, the first-order time-domain ordinary differential equation shown in Equation (1.20) needs to be discretized, which can be transformed into the discrete state-space equation as shown in Equation (1.24):

$$\begin{cases} U_0 = U_{ocv}\left(SOC_k\right) - U_{ct}\left(k\right) - r = R_0 I_0\left(k\right) \\ U_{ct}\left(k\right) = e^{-\frac{T}{R_{ct}C_{ct}}} U_{sf}\left(k-1\right) + \left(1 - e^{-\frac{T}{R_{ct}C_{ct}}}\right) R_{ct} I_0\left(k-1\right) \end{cases} \tag{1.24}$$

A fifth-degree polynomial equation is employed to depict the interplay between the open-circuit voltage (U_{ocv}) and the State of Charge (SOC), where SOC serves as the input and voltage emerges as the output in the battery. The model's construction takes place within the MATLAB/Simulink environment, followed by an in-depth simulation analysis. A visual representation of the first-order RC model's simulation platform is depicted in Figure 9.

5.2 Construction of the Second-Order RC Model Simulation Platform

The development of the simulation platform for the

second-order RC equivalent circuit model parallels that of the first-order model, both entailing an SOC assessment unit, a model parameter section, and an output validation component, depicted in Figure 10. Despite identical structures in their SOC estimation parts, the remaining two modules exhibit variations in parameter identification processes and functional relation expressions, catering to distinct purposes. Specifically, the output validation module unique to the second-order RC equivalent circuit model computes the voltage at the terminals corresponding to this model, which is then discharged as the simulation outcome.

Before constructing the simulation platform for the second-order RC equivalent circuit model in MATLAB/Simulink, the second-order time-domain ordinary differential equation needs to be discretized, which can be transformed into a discrete state-space equation:

$$\begin{cases} U_0 = U_{ocv}\left(SOC_k\right) - U_{sf}\left(k\right) - U_{ct}\left(k\right) - R_0 I_0\left(k\right) \\ U_{sf}\left(k\right) = e^{-\frac{T}{R_{sf}C_{sf}}} U_{sf}\left(k-1\right) + \left(1 - e^{-\frac{T}{R_{sf}C_{sf}}}\right) R_{sf} I_0\left(k-1\right) \\ U_{ct}\left(k\right) = e^{-\frac{T}{R_{ct}C_{ct}}} U_{sf}\left(k-1\right) + \left(1 - e^{-\frac{T}{R_{ct}C_{ct}}}\right) R_{ct} I_0\left(k-1\right) \end{cases} \tag{1.25}$$

The interplay between the open-circuit voltage, denoted as U_{ocv}, and U_{ocv} in terms of SOC is depicted through a quintic polynomial equation. SOC assumes the role of the input variable, whereas voltage serves as the output within the battery simulation model constructed in MATLAB/Simulink. A visual representation of the second-order RC model's simulation platform is depicted in Figure 11.

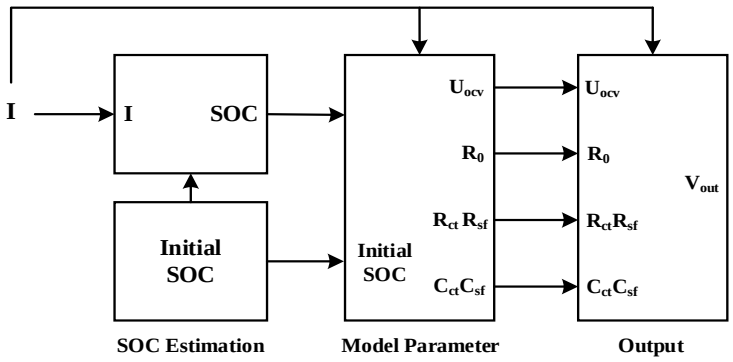

Figure 10 Schematic diagram of the second-order RC equivalent circuit model simulation platform

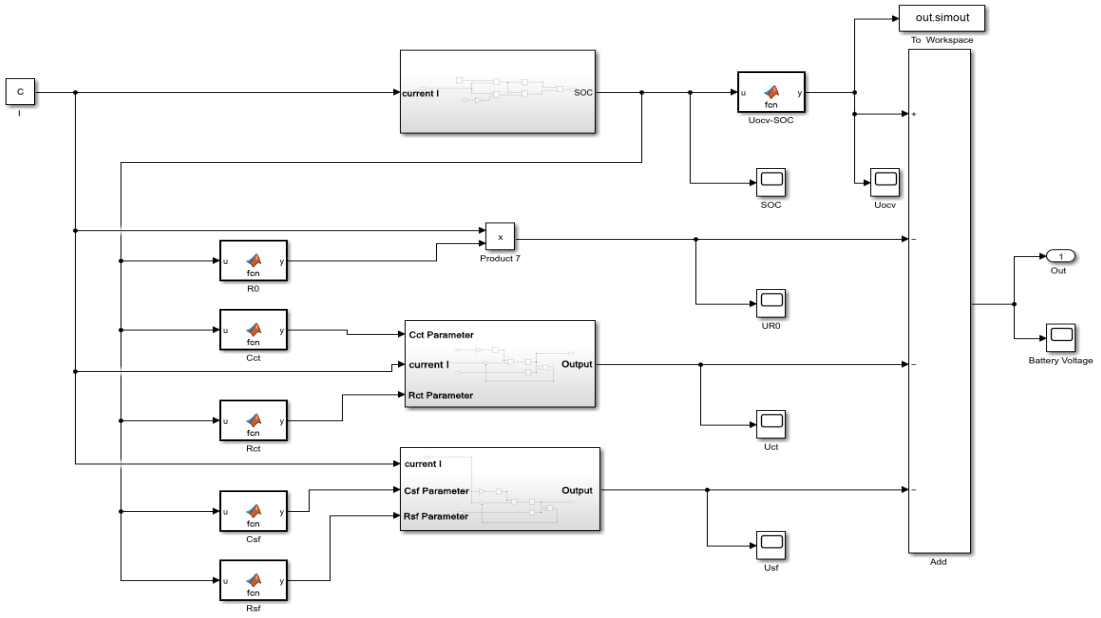

Figure 11 Simplified depiction of a simulation platform for the second-order RC circuit model

6. Model Simulation Verification

6.1 First-Order RC Model Simulation Verification

A constant current discharge test was carried out on the LSB cell at 0.1C rate under an ambient temperature of 25°C to yield experimental terminal voltage data. This data was subsequently juxtaposed with the simulated terminal voltage derived from the battery's first-order RC equivalent circuit model. As depicted in Figures 12 and 13, which illustrate the comparison curve and output error graph respectively, the first-order RC circuit model demonstrates high fitting precision. Throughout the discharge process, the majority of discrepancies are minimal, with the average error remaining below 0.9%. The peak voltage error transpires towards the conclusion of the discharge, yet it stays within the bounds of 3.0%. Overall, the mean interval error averages 19.7 mV, indicating a substantial level of consistency.

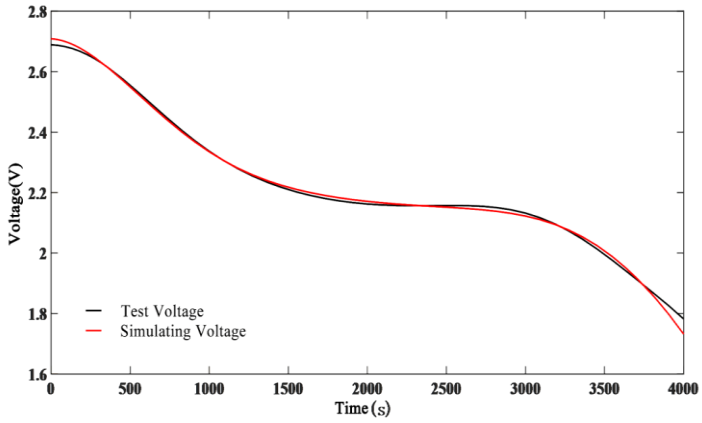

Figure 12 Comparison chart of terminal voltage between first-order RC model simulation and experimental test

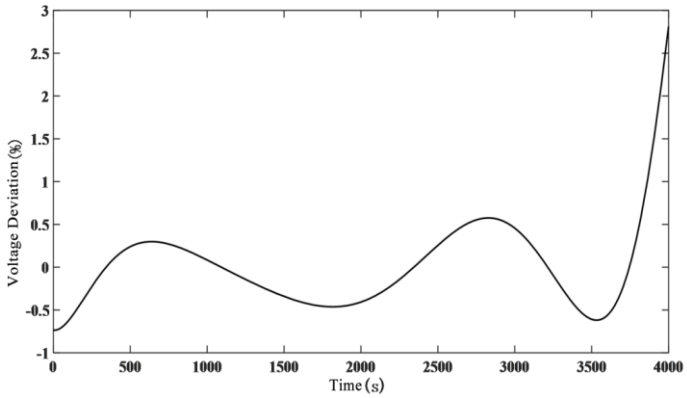

Figure 13 Voltage error curve chart of the first-order RC model simulation output

6.2 Second-Order RC Model Simulation Verification

Figures 14 and 15 respectively exhibit the comparative curve and output deviation graph of the terminal voltage between the simulation output of the second-order RC equivalent circuit model and the experimentally tested terminal voltage. Evidently from the illustrations, the fitting precision of the second-order RC equivalent circuit model is exceptionally high, as the discrepancies during the discharge phase remain below 0.9%. The minimum error of 0.5% is observed within the discharge period, while the peak error of 0.9% takes place at the conclusion of the discharge. Over the entire duration, the average error stands at 4.3 mV.

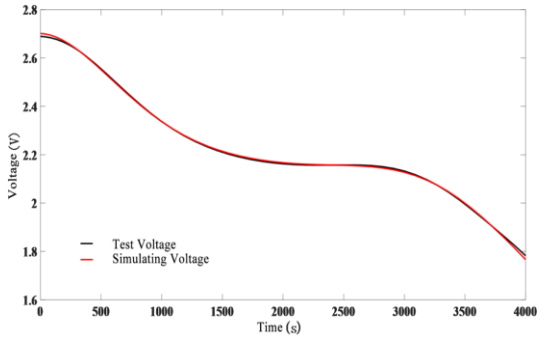

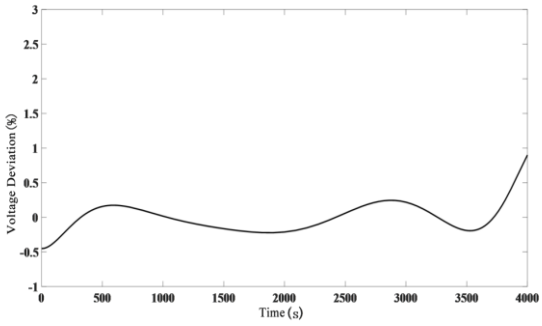

Figure 14 Comparison chart of terminal voltage between second-order RC model simulation and experimental test

Figure 15 Voltage error curve chart of the second-order RC model simulation output

An assessment of the simulation accuracy for the primary and subsequent RC parallel circuit renditions reveals comparable degrees of fidelity for both approaches. However, it is noteworthy that the second-order model demonstrates superior simulation efficiency. This distinction can be predominantly attributed to the distinct electrochemical behaviors intrinsic to LSB, especially during the discharge process, where the battery encounters electrode interface resistances and charge transfer impedances.These complex reaction mechanisms are reflected in the impedance spectrum in Figure 2. As a result, the first-order RC model, which includes only one set of parallel RC circuits, is insufficient to fit the increased polarization voltage, leading to parameter distortion and a decrease in fitting accuracy. Moreover, the increased error at the end of discharge can be attributed to the poor ionic conductivity of the end products Li_2S_2 and Li_2S, which form a significant reaction resistance within the battery, thereby causing a larger simulation error in the model during this phase.

7. Conclusions

Through extensive exploration of electrochemical impedance fundamentals and equivalent circuit components, we devised first- and second-order RC circuit models tailored to LSB impedance characteristics at varying SOC levels. Experimental findings from electrochemical tests and discharge procedures were utilized to parameterize these models, facilitating their efficient construction. To authenticate the efficacy of these equivalent circuit representations under constant current discharge scenarios, we executed simulations on a MATLAB/Simulink framework. The simulation outcomes confirmed the models' capability to reproduce LSB discharge dynamics accurately. The first-order RC model exhibited a simulation error margin of under 3%, while the second-order RC model surpassed this with an error below 0.9%, highlighting its superior precision in capturing the discharge kinetics of LSB. Consequently, the second-order RC model emerges as the more favorable option for battery modeling. By employing these models, we can predict battery discharge behavior with heightened accuracy, thereby furnishing a strong theoretical foundation for yacht battery management system design and enhancement.

Acknowledgment

This work was funded by Hainan Tropical Ocean College Talent Research Launch Project （RHDRC202310）; Education Department of Hainan Province（Hnjg2024ZD-44）; National Natural Science Foundation of China (51609131)

References

[1] M. Gaiotti, M. Aguiari, G. Vergassola, C.M. Rizzo et al. A rational approach for the scantling design of GRP pleasure crafts, Ocean Engineering, 2024, 304, 117866.

[2] Kang Y.,Pei Z.,Ao L.,Wu W..Reliability-based design optimization of river-sea-going ship based on agent model technology[J].Marine structures,2024,94(Mar.):1.1-1.19.

[3] Kujala P, Bergström M, Hirdaris S. Goal-based Ship Design Towards Safe and Sustainable Shipping in Ice-Covered Waters[J]. Transportation Research Procedia, 2023, 72: 3956-3963.

[4] Zheng Q, Yin X, Zhang D. State-space modeling for electrochemical performance of Li-ion batteries with

physics-informed deep operator networks[J]. Journal of Energy Storage, 2023, 73: 109244.

[5] Shateri N, Shi Z, Auger D J, et al. Lithium-sulfur cell state of charge estimation using a classification technique[J]. IEEE Transactions on Vehicular Technology, 2020, 70(1): 212-224.

[6] Chauque S, Souza B L, Sintaku H M, et al. Unveiling the polysulfide-PPY interaction for enhanced lithium–sulfur battery performance[J]. Electrochimica Acta, 2024, 475: 143539.

[7] Santos É A, Fernandes R C, Vicentini R, et al. On the electrochemical properties of lithium-sulfur batteries[J]. Journal of Energy Storage, 2023, 71: 108203.

[8] Hoseyni S M, Aghakhani A, Basdogan I. Experimental admittance-based system identification for equivalent circuit modeling of piezoelectric energy harvesters on a plate[J]. Mechanical Systems and Signal Processing, 2024, 208: 111016.

[9] Li A G, West A C, Preindl M. Characterizing degradation in lithium-ion batteries with pulsing[J]. Journal of Power Sources, 2023, 580: 233328.

[10] Huang H, Bian C, Wu M, et al. A novel integrated SOC–SOH estimation framework for whole-life-cycle lithium-ion batteries[J]. Energy, 2024, 288: 129801.

[11] Dini P, Colicelli A, Saponara S. Review on modeling and soc/soh estimation of batteries for automotive applications[J]. Batteries, 2024, 10(1): 34.

[12] Çarkıt T, Alçı M. Investigation of V oc and SoH on Li-ion batteries with an electrical equivalent circuit model using optimization algorithms[J]. Electrical Engineering, 2024, 106(2): 1781-1792.

[13] Watanabe H, Sugiura Y, Shitanda I, et al. Faradaic impedance and discharge reactions in lithium sulfur battery with sparingly solvating electrolyte[J]. Electrochimica Acta, 2024, 477: 143759.

[14] Zabara M A, Katırcı G, Civan F E, et al. Insights into charge transfer dynamics of Li batteries through temperature-dependent electrochemical impedance spectroscopy (EIS) utilizing symmetric cell configuration[J]. Electrochimica Acta, 2024, 485: 144080.

[15] Babaeiyazdi I, Rezaei-Zare A, Shokrzadeh S. State of charge prediction of EV Li-ion batteries using EIS: A machine learning approach[J]. Energy, 2021, 223: 120116.

[16] Li C, Yang L, Li Q, et al. SOH estimation method for lithium-ion batteries based on an improved equivalent circuit model via electrochemical impedance spectroscopy[J]. Journal of Energy Storage, 2024, 86: 111167.

[17] Li F, Zuo W, Zhou K, et al. State-of-charge estimation of lithium-ion battery based on second order resistor-capacitance circuit-PSO-TCN model[J]. Energy, 2024, 289: 130025.

[18] Zhao J, Qahouq J A A. Modeling and validation for performance analysis and impedance spectroscopy characterization of lithium-ion batteries[J]. Next Energy, 2024, 5: 100153.

[19] Tolouei N E, Ghamari S, Shavezipur M. Development of circuit models for electrochemical impedance spectroscopy (EIS) responses of interdigitated MEMS biochemical sensors[J]. Journal of Electroanalytical Chemistry, 2020, 878: 114598.

[20] Lipu M S H, Ansari S, Miah M S, et al. Deep learning enabled state of charge, state of health and remaining useful life estimation for smart battery management system: Methods, implementations, issues and prospects[J]. Journal of Energy Storage, 2022, 55: 105752.

Received **30 June 2024**

Accepted **02 July 2024**